Communication

Elimination of Dual Slope from the Coffin–Manson Relationship of Low-Cycle Fatigue in the Titanium Alloy Timetal 834, by Cold Rolling

K.V. SAI SRINADH and VAKIL SINGH

Cold rolling of the titanium alloy Timetal 834 was found to cause marked enhancement in low-cycle fatigue (LCF) life at low strain amplitude and to eliminate bilinear behavior from the Coffin–Manson (C-M) relationship. It was due to work hardening of surface grains of soft orientation and consequent increase in resistance of the material against crack initiation. The observed effect was not associated with texture.

DOI: 10.1007/s11661-007-9229-z

Alloy Timetal 834 is a near α-titanium alloy designed for high-temperature applications as compressor disc and blade of advanced gas turbines of jet engines, to substitute the heavy nickel-base super alloys. It is already in use for some applications where temperature excursions reach even up to 923 K.[1] Because the service conditions of the structural components such as compressor discs and turbine blades involve monotonic as well as cyclic loading, a combination of both high creep strength and fatigue resistance is required for their satisfactory working. For optimum performance of the alloy Timetal 834, a bimodal microstructure with 10 to 15 vol pct of primary α, in a lamellar matrix of transformed β, has been established.[2,3]

Srinadh and Singh[4] have recently characterized the cyclic stress response and low-cycle fatigue (LCF) behavior of Timetal 834 in the ($\alpha + \beta$) solution-treated, air-cooled, and stabilized condition, at a constant strain rate of 0.008 s^{-1} and at room temperature, and observed a bilinear behavior in the Coffin–Mansion (C-M) relationship. The lower segment of the C-M plot, corresponding to the region of low strain amplitudes, was found to be much steeper than that of the upper one. Likewise, fatigue life, at the lower strain amplitudes ($\Delta\varepsilon_p/2 < \pm 0.131$ pct), was considerably less than that expected from extrapolation of the upper segment. Similar dual slope in the C-M plot of this alloy has been established also at a constant cyclic frequency of 0.2 Hz (5). The lower fatigue life, at low strain amplitudes, was established to be associated with localization of plastic strain in a few widely spaced planar slip bands in the surface grains of soft orientations and consequent enhancement in the process of fatigue crack initiation in them.[5]

In view of the previous observations, the present investigation was undertaken to work harden the surface grains of soft orientation by cold rolling and to examine its effect on the C-M relationship of the alloy Timetal 834.

Alloy Timetal 834 was procured from M/s Imperial Metal Industries (MFD BY Timet, Birmingham, UK) in the form of rods of 18-mm diameter. It contained (mass pct) Al-5.07 pct, Sn-3.08 pct, Zr-3.45 pct, Nb-0.66 pct, Mo-0.31 pct, Si-0.2 pct, C-0.04 pct, O-0.075 pct, and balance Ti. Blanks of 100-mm length were vacuum (10^{-3} torr) sealed in a silica tube, solution treated in the $\alpha + \beta$ phase field at 1283 K for 1 hour, and cooled in air. These blanks were aged at 973 K for 2 hours and cooled in air to stabilize the microstructure. This heat treatment is thus designated as ($\alpha + \beta$) ST-AC-A. The heat-treated blanks were cold rolled using a laboratory-type rolling mill with circular roll pass, and the cross-sectional area of the blanks was reduced by 15 pct. Mechanically polished samples were etched with a solution of 10 HF + 5 HNO_3 + 85 H_2O (vol pct) for optical microscopy.

Standard Hounsfield tensile specimens, with gage length and diameter of 15.4 and 4.52 mm, respectively, were machined and tested at a strain rate of 5.4×10^{-4} s^{-1} using a screw-driven Instron of 50 kN capacity (INSTRON TT-CM-L, Boston, USA).

The effect of cold rolling on preferred orientation was studied by texture analysis using the Panalytical MRD system (MRD Panalytical, Enidhoven, Netherland). Flat samples of $22 \times 10 \times 3$ mm size were machined from the midsections of both as-received and cold-rolled blanks for texture study. These samples were polished first mechanically and then electrolytically before texture analysis.

The LCF tests were performed using cylindrical specimens, with gage length and diameter of 15 and 5.5 mm, respectively, shoulder radii of 25 mm, and threaded ends of 35-mm length and 12-mm diameter on either side. The gage section of the machined LCF specimens was mechanically polished with emery papers of 1/0 to 4/0 grades and finally by slurry of 0.3 μ alumina powder in water, to minimize the surface effect, if any. The LCF tests were performed under total strain control mode, in fully reversed axial loading ($R = -1$), at a constant strain rate of 0.008 s^{-1}, using a servo hydraulic MTS of ± 50 kN, equipped with a "Test star" software system. Strain was monitored by a 10-mm gage length extensometer (model number 632.13C-20), and the cyclic load was applied in triangular wave form. Failure was considered as a 15 pct drop in the load corresponding to that at the 100th cycle.

The optical microstructure of the alloy Timetal 834 in the as heat-treated condition [($\alpha + \beta$) ST-AC-A] and in the 15 pct cold-rolled condition is shown in Figures 1(a) and (b), respectively. It is obvious that the microstructure

K.V. SAI SRINADH, Assistant Professor, is with the Department of Mechanical Engineering, National Institute of Technology, Warangal 506 002, India. VAKIL SINGH, Professor, is with the Centre of Advanced Studies, Department of Metallurgical Engineering, Institute of Technology, Banaras Hindu University, Varanasi 221005, India. Contact e-mail: vakil@bhu.ac.in
Manuscript submitted February 5, 2007.
Article published online July 14, 2007.

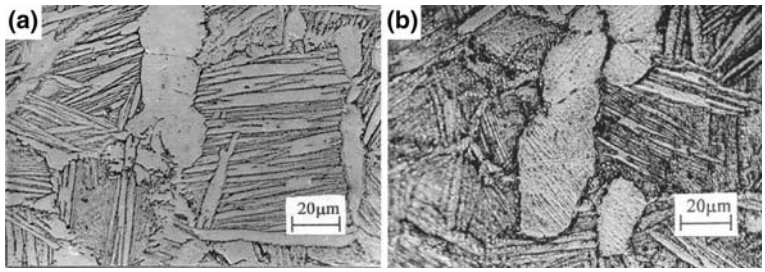

Fig. 1—Optical microstructure of the alloy Timetal 834: (*a*) as heat treated and (*b*) 15 pct cold rolled.

is bimodal in nature and that the volume fraction of the primary α-phase is approximately 12 pct. In general, the microstructural features of the as-heat-treated and cold-rolled material are comparable, except the appearance of distinct slip traces, particularly in the primary α phase, of the cold-worked material (Figure 1). Fine slip traces may be seen also in the transformed β phase of the cold-worked material. Tensile properties of the alloy in the as-heat-treated as well as cold-rolled condition are recorded in Table I.

While the strength parameters (yield strength σ_{ys}, ultimate tensile strength σ_{UTS}, and strength coefficient K) are relatively higher, the degree of work hardening ($\sigma_{\text{UTS}}/\sigma_{YS}$) and the work-hardening exponent (n) are relatively lower in the cold-rolled condition. The ductility parameters (uniform elongation (e_u), total elongation (e_t), and reduction in area (RA)) are considerably lower in the cold-rolled condition.

Cyclic softening was observed both in the as-heat-treated and in the cold-rolled condition. However, the degree of softening was found to be relatively higher in the as-heat-treated condition than that in the cold-rolled one. The LCF behavior was analyzed using the C-M relationship between the plastic strain amplitude ($\Delta\varepsilon_p/2$) and the number of reversals to failure ($2N_f$):

$$\Delta\varepsilon_p/2 = \varepsilon'_f(2N_f)^c \qquad [1]$$

where ε'_f and c are the fatigue ductility coefficient and fatigue ductility exponent, respectively. It is evident that while there is only one slope in the cold-worked condition, there are two slopes in the as-heat-treated condition (Figure 2).

The other fatigue parameters (fatigue strength coefficient (σ'_f) and fatigue strength exponent (b)) were evaluated using the Basquin's relationship between the elastic strain amplitude ($\Delta\varepsilon_e/2$) and the number of reversals to failure:

$$\Delta\varepsilon_{e/2} = (\sigma'/E) \times (2N_f)^b \qquad [2]$$

where E is the Young's modulus. Transition fatigue life (N_t) was determined at the point of intersection of the elastic and plastic strain amplitude plots. The values of the fatigue parameters and transition fatigue life are recorded in Table II. It is obvious that the experimentally determined fatigue ductility exponent (c_{exp}) for the 15 pct cold-rolled condition is relatively closer to the generally observed value (−0.5 to −0.6) as compared to that of the as-heat-treated one. On the other hand, the value of the experimentally determined fatigue strength exponent (b_{exp}) is lower for the cold-rolled condition than the as heat-treated one. The fracture behavior of the as-heat-treated and 15 pct cold-rolled material, tested in LCF at $\Delta\varepsilon_t/2$: ±0.7 pct, is shown by scanning electron microscopy (SEM) fractographs in Figure 3.

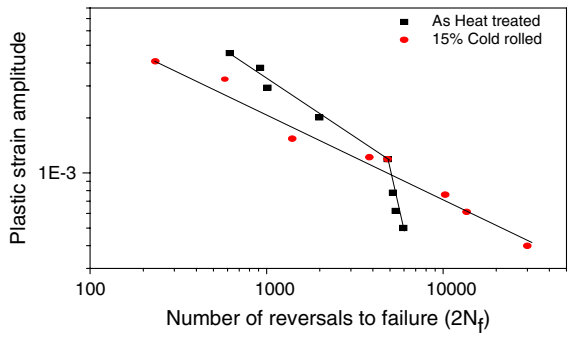

Fig. 2—C-M plot for the alloy Timetal 834.

Table I. Tensile Properties of the Alloy Timetal 834 in the As-Heat-Treated and 15 Pct Cold-Rolled Condition

Tensile Properties	Heat Treated	Cold Rolled
σ_y	929 (MPa)	1133 (MPa)
σ_{UTS}	1014 (MPa)	1161 (MPa)
$\sigma_{\text{UTS}}/\sigma_{YS}$	1.09	1.02
e_u	10.1 (pct)	2.5 (pct)
e_f	13.3 (pct)	5.8 (pct)
RA	12 (pct)	8 (pct)
n	0.06	0.04
K	1263 (MPa)	1354 (MPa)

Table II. Fatigue Parameters and Transition Fatigue Life in As-Heat-Treated and 15 Pct Cold-Rolled Condition

Fatigue Parameters	As Heat Treated	15 Pct Cold Rolled
c_{exp}	−0.61	−0.49
c_{cal} $-1/(1 + 5n')$	−0.74	−0.80
ε'_f	0.35	0.30
b_{exp}	−0.075	−0.065
b_{cal} $-n'/(1 + 5n')$	−0.06	−0.05
σ'_f	1200 MPa	1254 MPa
N_t	115 cycles	38 cycles

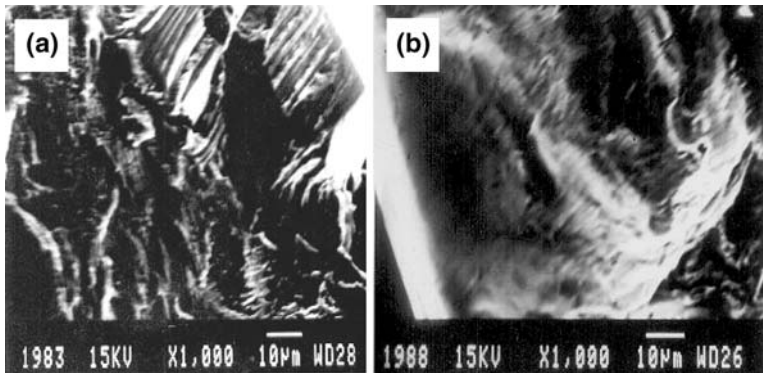

Fig. 3—SEM fractographs showing fracture behavior of the LCF specimen, tested at $\Delta\varepsilon_t/2 \leq \pm 0.7$ pct, at room temperature: (*a*) as heat treated and (*b*) 15 pct cold rolled.

Various mechanisms, such as the change in the mode of fracture with increase in strain amplitude,[6,7] environmentally assisted fatigue degradation,[8,9] and change in deformation behavior through work-hardening characteristics,[10] have been proposed for bilinear behavior in the C-M relationship. However, bilinearity in the C-M relationship of the alloy 834, in the ($\alpha + \beta$) ST-AC-A condition, has been found to be associated with the difference in the mode of deformation at low and high strain amplitudes.[5] The much lower fatigue life of the alloy Timetal 834 in the as-heat-treated condition, at low strain amplitudes ($\Delta\varepsilon_p/2 < \pm 0.131$ pct), than that expected from extrapolation of the upper segment of the C-M plot may be attributed to early fatigue crack initiation, resulting from localization of plastic strain in a few planar slip bands, in the favorably oriented surface grains, as established in our earlier investigation.[5]

It may be seen that there is marked influence of cold rolling on fatigue life, particularly at the low strain amplitudes ($\Delta\varepsilon_p/2 < \pm 0.131$ pct). Cold rolling enhances the fatigue life by a factor of 5 at the lowest strain amplitude ($\Delta\varepsilon_p/2$: ± 0.057 pct). It is known that fatigue life at low strain amplitudes is controlled essentially by resistance of material against the process of fatigue crack initiation. Fatigue crack initiation, at low strain amplitudes, in the as-heat-treated condition, is enhanced by the planarity of slip and localization of plastic strain in a few widely spaced slip bands. However, when the heat-treated blanks are cold rolled, the grains of soft orientations, exhibiting planar slip, undergo heavy plastic deformation and work harden due to activation of other variance of slip and additional slip systems. Thus, the regions of soft orientations, with favorable orientations for planar slip, are eliminated following cold rolling and the resistance of the material against fatigue crack initiation, at low strain amplitudes, is markedly enhanced. Parallel slip bands may clearly be seen across the width of the primary α grains at the surface of the heat-treated specimen (Figure 4(a)) tested at $\Delta\varepsilon_p/2 \pm 0.057$ pct. In sharp contrast, no such slip bands are seen in the cold-rolled material (Figure 4(b)), tested under identical conditions. Planar slip bands in the primary α phase of the as-heat-treated material may be seen more clearly in the SEM micrograph (Figure 5). The dark regions parallel to slip bands are potential sites for crack initiation. Deformation of primary α phase in the heat-treated material, in widely spaced coarse slip bands, is promoted by shearing of coherent and ordered α_2 precipitates in that condition.[11,12] High planarity of slip, in the as-heat-treated condition, particularly in the primary α phase, may be seen to affect also the fracture behavior (Figure 3). While there are faceted features at the site of fatigue crack initiation in the case of the as-heat-treated material, in the cold-rolled material, there

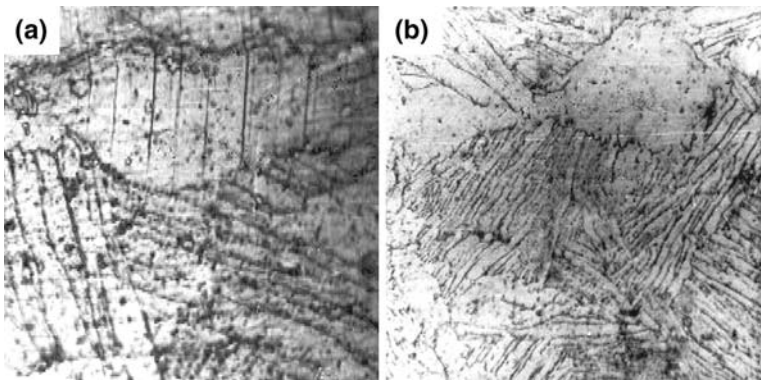

Fig. 4—Optical micrographs showing surface features, following LCF at $\Delta\varepsilon_p/2 \pm 0.057$ pct, at room temperature: (*a*) as-heat-treated material showing planar slip bands in primary α and (*b*) 15 pct cold-rolled material without such features.

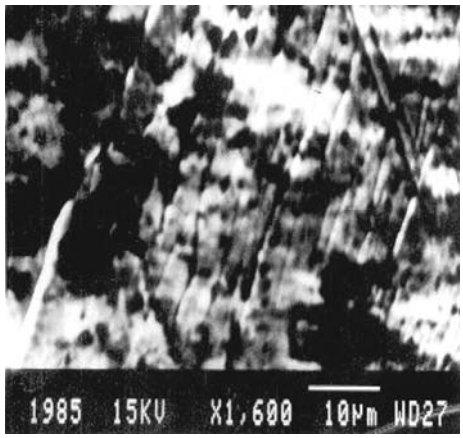

Fig. 5—SEM micrograph showing distinct planar slip bands in primary α phase at surface, in gage section, following LCF at $\Delta\varepsilon_t/2$: ± 0.7 pct, at room temperature.

are distinct fatigue striations. The faceted features in the circumferential region of the fracture surface of the as-heat-treated material may be understood in light of the earlier investigation[12] on fatigue crack initiation in the primary α phase of this alloy, by pileup of dislocations on basal plane at barriers, and consequent initiation and growth of cracks along the weak cleavage planes. In contrast, the absence of faceted features in the cold-rolled material may be attributed to the much lower tendency of planar slip in this condition because of the more uniform deformation due to activation of additional slip systems and consequent extensive fragmentation of the ordered α_2 precipitates.

It was observed from the texture study that the orientation distribution function (ODF) intensity was higher (4.422) for the as-heat-treated condition than that of the cold-rolled one (2.345). Thus, there is no correlation between the texture and the slope of the C-M plot. In fact, the orientation distribution function intensity has decreased as a result of cold rolling. The enhancement in LCF resistance of the material, as a result of cold rolling, at low strain amplitudes, is due to strengthening of surface grains of soft orientation. On the other hand, the deleterious effect of cold rolling on fatigue life, at high strain amplitudes ($\Delta\varepsilon_p/2 \geq \pm 0.131$ pct), may be attributed to exhaustion of ductility of the material (Table I), as observed in the HSLA[13,14] and 304 LN[15,16] steels.

Alloy Timetal 834 in the ($\alpha + \beta$) ST-AC-A condition exhibits dual slope behavior in the C-M plot. Obviously, the fatigue life in the region of low strain amplitude is much lower than that expected from extrapolation of the data of high strain amplitude. Fatigue life is markedly enhanced at low strain amplitude due to cold rolling, and consequently, the dual slope is eliminated from the C-M plot. The dual slope in the as-heat-treated condition occurs due to the planarity of slip and localization of strain in a few slip bands. The elimination of dual slope from cold rolling is attributed to strengthening of the surface grains of soft orientation and consequent inhibition of planarity of slip.

The authors are thankful to Dr. A.K. Gogia, Director, Project Office Materials, Kaveri Engine Programme, Hyderabad, for supplying of the alloy and for his interest in the work.

REFERENCES

1. S. Hardt, H.J. Mair, and H.J. Christ: *Int. J. Fat.*, 1999, vol. 21, pp. 779–89.
2. S. Hardt, H.J. Mair, and H.J. Christ: *Proc. Low Cycle Fatigue and Elastic-Plastic Behaviour of Materials*, Elsevier, Amsterdam, 1998, pp. 9–14.
3. D.F Neal: *Titanium Science and Technology: Proc. 5th Int. Conf. on Titanium Congress-Centre*, Munich, Sept. 10–14, 1984, DGM, Oberusel, 1985, pp. 2419–24.
4. K.V. Sai Srinadh and V. Singh: *Proc. 4th Conf. on Creep*, Fatigue and Creep-Fatigue Interaction, IGCAR, Kalpakkam, 2003, pp. C45–C49.
5. N. Singh, Gouthama, and V. Singh: *Mater. Sci. Eng. A*, 2002, vol. 325, pp. 324–32.
6. L.F. Coffin: *J. Mater.*, 1971, vol. 6, pp. 388–402.
7. N. Eswara Prasad, G. Malakondaiah, K.N. Raju, and P. Rama Rao: *Advances in Fracture Research*, ICF7, Houston, USA, 1989, p. 1103.
8. L.F. Coffin: *Metall. Trans. A*, 1972, vol. 13A, pp. 1777–88.
9. T.H. Sanders and E.A. Starke: *Metall. Mater. Trans. A*, 1996, vol. 27A, pp. 1407–12.
10. V. Singh, M. Sunderaraman, W. Chen, and R.P. Wahi: *Metall. Trans. A*, 1991, vol. 22, pp. 499–506.
11. G. Lutjering and S. Weissman: *Acta Metall.*, 1970, vol. 18, pp. 785–95.
12. G.J. Baxter, W.M. Rainforth, and L. Graboswski: *Acta Mater.*, 1996, vol. 44, pp. 3453–63.
13. S.K. Garg, V. Singh, and P. Rama Rao: *Scripta Metall.*, 1977, vol. 11, pp. 593–96.
14. D. Aichbhaumik: *Metall. Trans. A*, 1979, vol. 10A, pp. 269–78.
15. S.G. Sundara Raman and K.A. Padmanabhan: *Int. J. Fatigue*, 1996, vol. 18, pp. 71–79.
16. K. Bhanu Sankara Rao, M. Valsan, R. Sandhya, and S.L. Mannan: *Metall. Mater. Trans. A*, 1993, vol. 24A, pp. 913–17.